Spectrochimica Acta Part A: Molecular and Biomolecular Spectroscopy 136 (2015) 1418–1427

Contents lists available at ScienceDirect

Spectrochimica Acta Part A: Molecular and Biomolecular Spectroscopy

journal homepage: www.elsevier.com/locate/saa

DNA cleavage, antimicrobial studies and a DFT-based QSAR study of new antimony(III) complexes as glutathione reductase inhibitor

Turgay Tunç [a], Yasemin Koç [b], Leyla Açık [c], Mehmet Sayım Karacan [d], Nurcan Karacan [d,*]

[a] Ahi Evran University, Science Faculty, Chemistry Department, Kirsehir, Turkey
[b] Ankara University, Science Faculty, Biology Department, Ankara, Turkey
[c] Gazi University, Science Faculty, Biology Department, Ankara, Turkey
[d] Gazi University, Science Faculty, Chemistry Department, Ankara, Turkey

HIGHLIGHTS

- Fourteen new antimony(III) complexes were synthesized.
- Their structures were optimized by DFT/B3LYP/LANL2DZ method.
- DNA cleavage, antimicrobial activities and glutathione reductase inhibitor activities were screened.
- 2D-QSAR analyses were carried out for glutathione reductase inhibitory activities.

GRAPHICAL ABSTRACT

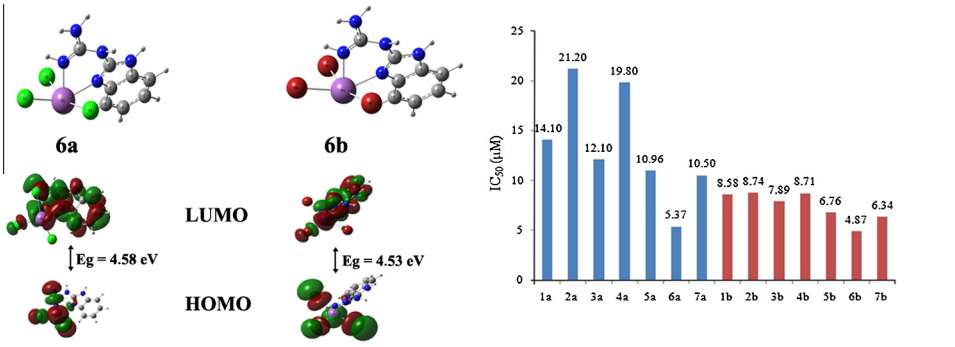

ARTICLE INFO

Article history:
Received 24 July 2014
Received in revised form 16 September 2014
Accepted 13 October 2014
Available online 19 October 2014

Keywords:
Antimony(III) complexes
QSAR
Glutathione reductase inhibitors
DNA cleavage activity antimicrobial activity

ABSTRACT

New antimony(III) complexes, [Sb(2-aminopyridine)$_2$Cl$_3$] (1a), [Sb(2-aminopyridine)$_2$Br$_3$] (1b), [Sb(5-methyl-2-aminopyridine)$_2$Cl$_3$] (2a), [Sb(5-methyl-2-aminopyridine)$_2$Br$_3$] (2b), [Sb(2-aminopyrimidine)$_2$Cl$_3$] (3a), [Sb(2-aminopyrimidine)$_2$Br$_3$] (3b), [Sb(4,6-dimethoxy-2-aminopyrimidine)$_2$Cl$_3$] (4a), [Sb(4,6-dimethoxy-2-aminopyrimidine)$_2$Br$_3$] (4b), [Sb(2-amino-1,3,5-triazine)$_2$Cl$_3$] (5a), [Sb(2-amino-1,3,5-triazine)$_2$Br$_3$] (5b), [Sb(2-guanidinobenzimidazole) Cl$_3$] (6a), [Sb(2-guanidinobenzimidazole)Br$_3$] (6b) [Sb(2- benzyl-2-thiopseudeourea)$_2$Cl$_3$] (7a) and [Sb(2- benzyl-2-thiopseudeourea)$_2$Br$_3$] (7b) were synthesized. Their structures were characterized by elemental analysis, molecular conductivity, FT-IR, ^{1}H NMR, LC–MS techniques. Glutathione reductase inhibitor activity, antimicrobial activity and DNA cleavage studies of the complexes were determined. The geometrical structures of the complexes were optimized by DFT/B3LYP method with LANL2DZ as basis set. Calculation results indicated that the equilibrium geometries of all complexes have square pyramidal shape. About 350 molecular descriptors (constitutional, topological, geometrical, electrostatic and quantum chemical parameters) of the complexes were calculated by DFT/B3LYP/LANL2DZ method with CODESSA software. Calculated molecular parameters were correlated to glutathione reductase inhibitory activity values (pIC$_{50}$) of all complexes by Best Multi-Linear Regression (BMLR) method. Obtained two-parameter QSAR equation shows that increase in "maximum partial charge for a H atom" and decrease in HOMO–LUMO gap would be favorable for the glutathione reductase inhibitory activity.

* Corresponding author. Tel.: +90 312 2021117; fax: +90 312 2122279.
E-mail address: nkaracan@gazi.edu.tr (N. Karacan).

http://dx.doi.org/10.1016/j.saa.2014.10.030
1386-1425/

Introduction

Glutathione reductase is a key enzyme in the maintenance of GSH/GSSG ratio, by catalyzing the conversion of oxidized glutathione (GSSG) to the reduced form (GSH). This biochemical processes are essential for detoxification of free radicals and reactive oxygen species as well as DNA biosynthesis, protection of cells against various oxidative stresses, intra-cellular signal transduction, and gene regulation [1]. Glutathione reductase inhibitors are known to possess anticancer and antimalarial activity and they can enhance the effects of chloroquine or cytotoxic agents as drug sensitizers [2]. From a drug development perspective, inhibition of glutathione reductase enzyme is very important. Wyllie and Fairlamb reported that Sb(III) complexes, originally used in the treatment of leishmaniasis, inhibits glutathione reductase activity in macrophages and proposed it as a drug for acute promyelocytic leukemia [3]. To date, various organic-based glutathione reductase inhibitors were published in many articles [4] but a few metal-complex glutathione reductase inhibitors have been reported such as Au(I), Ag(I), Sb(III) and ferrocenic complexes [5–7].

Metal-containing drugs have growing importance in therapeutics and diagnostics, particularly in anticancer chemotherapy [8]. DNA binding properties of metal complexes also gains importance owing to their diverse applications as diagnostic agents for medical applications and cleavage agents for probing nucleic acid structure [9–11]. On the other hand, antimony complexes have various potential usage in the field of pharmacy [12,13] such as anthelmintic [14,15], antitrypanosomal [16], anticancer [17–20], antileishmanial [21–23] and antimicrobial [24–28] agents.

For the designing of new compounds with enhanced biological activity, quantitative structure-activity relationship (QSAR) has been an attractive approach by establishing correlation between chemical structure modifications and respective changes of biological activity [29]. As part of our ongoing QSAR studies [30–34], in the present work, we correlated the glutathione reductase inhibitory activity of new antimony(III) complexes So, we synthesized new fourteen antimony(III) complexes of N-donor ligands (2-aminopyridine, $C_5H_6N_2$; 5-methyl-2-aminopyridine, $C_6H_8N_2$; 2-aminopyrimidine, $C_4H_5N_3$; 4,6-dimethoxy-2-aminopyrimidine, $C_6H_9N_3O_2$; 2-amino-1,3,5-triazine, $C_3H_4N_4$; 2-guanidinobenzimidazole, $C_8H_9N_5$; 2-benzyl-2-thiopseudeourea, $C_8H_{10}N_2S$), $[Sb(2\text{-aminopyridine})_2Cl_3]$ (**1a**), $[Sb(2\text{-aminopyridine})_2Br_3]$ (**1b**), $[Sb(5\text{-methyl-2-aminopyridine})_2Cl_3]$ (**2a**), $[Sb(5\text{-methyl-2-aminopyridine})_2Br_3]$ (**2b**), $[Sb(2\text{-aminopyrimidine})_2Cl_3]$ (**3a**), $[Sb(2\text{-aminopyrimidine})_2Br_3]$ (**3b**), $[Sb(4,6\text{-dimethoxy-2-aminopyrimidine})_2Cl_3]$ (**4a**), $[Sb(4,6\text{-dimethoxy-2-aminopyrimidine})_2Br_3]$ (**4b**), $[Sb(2\text{-amino-1,3,5-triazine})_2Cl_3]$ (**5a**), $[Sb(2\text{-amino-1,3,5-triazine})_2Br_3]$ (**5b**), $[Sb(2\text{-guanidinobenzimidazole})Cl_3]$ (**6a**), $[Sb(2\text{-guanidinobenzimidazole})Br_3]$ (**6b**), $[Sb(2\text{-benzyl-2-thiopseudeourea})_2Cl_3]$ (**7a**) and $[Sb(2\text{-benzyl-2-thiopseudeourea})_2Br_3]$ (**7b**). Their structures were characterized by elemental analysis, molecular conductivity, FT-IR, ^1H NMR, LC–MS techniques. Glutathione reductase inhibitory activity, DNA cleavage activity and antimicrobial activity of all complexes were evaluated and discussed.

Experimental

Materials and methods

All chemicals used in this study were purchased from Sigma–Aldrich. All reagents were used without further purification. The NMR spectra were recorded in d_6-DMSO in a Bruker Ultrashield 300 MHz spectrometer. Elemental analyses were determined on a LECO CHNS–932 auto elemental analysis apparatus. The molecular conductivities of the complexes were measured with WTW Cond 330i. Infrared spectra were obtained by using a Mattson 1000 FT–IR Spectrometer, from 4000–400 cm^{-1} in KBr pellet. Liquid Chromatography Mass spectra were obtained by using a Platform LC–MS with methanol–acetonitrile mixture as the solvent.

Synthesis of the complexes

The complexes were prepared by the following general method [26]. 25 mL methanol solution of ligand was added to antimony(III) halides dissolved in the same solvent in the mole ratio of 2:1 in hydrochloric acid. The mixture was refluxed for 2 days at 60 °C, after that the mixture was concentrated to 1/3 of its initial volume and allowed to stand for crystallization at room temperature. The obtained colorless, yellow and pink crystals were filtered and dried in air.

*$[Sb(2\text{-aminopyridine})_2Cl_3]$ (**1a**)*

Anal. Calcd. for $C_{10}H_{12}Cl_3N_4Sb$: C, 28.85; H, 2.91; N, 13.46. Found: C, 28.17; H, 2.75; N, 13.97 IR (KBr, ν/cm^{-1}): 3442 (ν NH_2), 1661 (ν CC_{ring}), 1621 (ν CN_{ring}), 994 (ν CH_{ring}). LC–MS (MeOH): *m/z* [found (calcd)]: 418.34 (416.35) (M + 2): ^1H NMR (300 MHz, DMSO-d_6): Δ 2.50 (2H, NH_2), 7.95 (H_1, Ar), 7.90 (H_3, Ar), 6.98 (H_4, Ar), 6.86 (H_3, Ar), m.p. 174–175 °C, yield: 58.82%.

*$[Sb(2\text{-aminopyridine})_2Br_3]$ (**1b**)*

Anal. Calcd. for $C_{10}H_{12}Br_3N_4Sb$: C, 21.85; H, 2.20; N, 10.19. Found: C, 21.04; H, 2.71; N, 10.86. IR (KBr, ν/cm^{-1}): 3413 (ν NH_2), 1658 (ν CC_{ring}), 1620 (ν CN_{ring}), 1024 (ν CH_{ring}). LC–MS: *m/z* (calcd) = 549.70 (550.62) (M + 1): ^1H NMR (300 MHz, DMSO-d_6): Δ 2.50 (2H, NH_2), 7.95 (H_1, Ar), 7.90 (H_3, Ar), 6.98 (H_4, Ar), 6.86 (H_3, Ar), m.p. 177–178 °C, yield: 70.14%.

*$[Sb(5\text{-methyl-2-aminopyridine})_2Cl_3]$ (**2a**)*

Anal. Calcd. for $C_{12}H_{16}Cl_3N_4Sb$: C, 32.43; H, 3.63; N, 12.61. Found: C, 33.02; H, 3.82; N, 12.10. IR (KBr, ν/cm^{-1}): 3429 (ν NH_2), 3040 (ν CH), 1668 (ν CC_{ring}), 1625 (ν CN_{ring}). LC–MS: *m/z* (calcd) = 444.40 (444.86) (M+). ^1H NMR (300 MHz, DMSO-d_6): Δ 2.2 (3H, CH_3), 3.50 (2H, NH_2), 6.95 (H_6, Ar), 7.8 (H_5, Ar), 7.90 (H_1, Ar), m.p. 174–176 °C, yield: 87.12%.

*$[Sb(5\text{-methyl-2-aminopyridine})_2Br_3]$ (**2b**)*

Anal. Calcd. for $C_{12}H_{16}Br_3N_4Sb$: C, 24.95; H, 2.79; N, 9.70. Found: C, 25.43; H, 2.38; N, 9.12. IR (KBr, ν/cm^{-1}): 3419 (ν NH_2), 2930 (ν CH), 1668 (ν CC_{ring}), 1627 (ν CN_{ring}). LC–MS: *m/z* (calcd) = 579.75 (578.98) (M + 1). ^1H NMR (300 MHz, DMSO-d_6): Δ 2.3 (3H, CH_3), 3.50 (2H, NH_2), 7.00 (H_6, Ar), 7.80 (H_5, Ar), 7.90 (H_1, Ar), m.p. 175–177 °C, yield: 91.47%.

*$[Sb(2\text{-aminopyrimidine})_2Cl_3]$ (**3a**)*

Anal. Calcd. For $C_8H_{10}Cl_3N_6Sb$: C, 22.97; H, 2.41; N, 20.09. Found: C, 23.39; H, 2.71; N, 20.74. IR (KBr, ν/cm^{-1}): 3346 (ν NH_2), 1658 (ν CC_{ring}), 1619 (ν CN_{ring}), 990 (ν CH_{ring}). LC–MS: *m/z* (calcd) = 420.32 (419.35) (M + 1). ^1H NMR (300 MHz, DMSO-d_6): Δ 5.40 (2H, NH_2), 8.40 (H_1, H_3, Ar), 6.75 (H_2, Ar), m.p. 170–171 °C, yield: 62.50%.

*$[Sb(2\text{-aminopyrimidine})_2Br_3]$ (**3b**)*

Anal. Calcd. for $C_8H_{10}Br_3N_6Sb$: C, 17.42; H, 1.83; N, 15.23. Found: C, 17.96; H, 1.94; N, 15.74. IR (KBr, ν/cm^{-1}): 3320 (ν NH_2), 3155 (ν CH), 1684 (ν CC_{ring}), 1618 (ν CN_{ring}). LC–MS: *m/z* (calcd) = 551.68 (551.75) (M+). ^1H NMR (300 MHz, DMSO-d_6): Δ 5.40 (2H, NH_2), 8.60 (H_1, H_3, Ar), 7.00 (H_2, Ar), m.p. 172–173 °C, yield: %72.69.

*$[Sb(4\text{-}6\text{-dimethoxy-2-aminopyrimidine})_2Cl_3]$ (**4a**)*

Anal. Calcd. for $C_{14}H_{20}Cl_3N_4O_4Sb$: C, 26.77; H, 3.37; N, 15.61. Found: C, 27.11; H, 3.67; N, 15.96. IR (KBr, ν/cm^{-1}): 3391 (ν NH_2), 2940 (ν CH), 2909 (ν CH), 1684 (ν CC_{ring}), 1656 (ν CN_{ring}),

939 (ν CH_{ring}). LC–MS: *m/z* (calcd) = 540.43 (539.15) (M + 1). ^{1}H NMR (300 MHz, DMSO-d_6): Δ 3.50 (2H, NH_2), 4.90 (3H, OCH_3), 5.70 (1H, Ar), m.p. >400 °C, yield: 30.24%.

*[Sb(4-6-dimethoxy-2-aminopyrimidine)$_2$Br$_3$] (**4b**)*

Anal. Calcd. for $C_{14}H_{20}Br_3N_4O_4Sb$: C, 21.45; H, 2.70; N, 12.51. Found: C, 21.03; H, 2.17; N, 12.79. IR (KBr, ν/cm^{-1}): 3325 (ν NH_2), 2928 (ν CH), 2885 (ν $_{CH}$), 1674 (ν CC_{ring}), 1658 (ν CN_{ring}), 941 (ν CH_{ring}). LC–MS: *m/z* (calcd) = 673.78 (672.35) (M + 1). ^{1}H NMR (300 MHz, DMSO-d_6): Δ 3.60 (2H, NH_2), 5.10 (3H, OCH_3), 5.80 (1H, Ar), m.p. >400 °C, yield: 30.36%.

*[Sb(2-amino-1,3,5-triazine)$_2$Cl$_3$] (**5a**)*

Anal. Calcd. for $C_6H_8Cl_3N_8Sb$: C, 17.15; H, 1.92; N, 26.66. Found: C, 17.69; H, 2.08; N, 26.13. IR (KBr, ν/cm^{-1}): 1620 (ν CC_{ring}), 1562 (ν CN_{ring}), 1006 (ν CH_{ring}). LC–MS: *m/z* (calcd) = 421.78 (420.30) (M + 1). ^{1}H NMR (300 MHz, DMSO-d_6): Δ 6.80 (2H, NH_2), 8.75 (1H, Ar), 8.95 (1H, Ar), m.p. 174–176 °C, yield: 30.36%.

*[Sb(2-amino-1,3,5-triazine)Br$_3$] (**5b**)*

Anal. Calcd. for $C_6H_8Br_3N_8Sb$: C, 13.02; H, 1.46; N, 20.24. Found: C, 13.79; H, 1.73; N, 21.02. IR (KBr, ν/cm^{-1}): 1622 (ν CC_{ring}), 1563 (ν CN_{ring}), 1008 (ν CH_{ring}). LC–MS: *m/z* (calcd) = 554.16 (553.65) (M + 1). ^{1}H NMR (300 MHz, DMSO-d_6): Δ 6.90 (2H, NH_2), 8.80 (1H, Ar), 8.90 (1H, Ar), m.p. 174–176 °C, yield: 33.26%.

*[Sb(2-guanidinobenzimidazole)Cl$_3$] (**6a**)*

Anal. Calcd. for $C_8H_9Cl_3N_5Sb$: C, 23.82; H, 2.25; N, 17.36. Found: C, 23.37; H, 2.02; N 17.13. IR (KBr, ν/cm^{-1}): 3430 (ν NH_2), 3333 (ν NH), 3063 (ν CH_{ar}), 1689 (ν CC), 1629 (ν CN). LC–MS: *m/z* (calcd) = 404.08 (403.31) (M + 1): ^{1}H NMR (300 MHz, DMSO-d_6): Δ 11.90 (1H, NH), 8.20 (1H, NH), 7.40 and 7.20 (4H, Ar), 6.40 (3H, NH_2 and NH), m.p. 217–218 °C, yield: 53.22%.

*[Sb(2-guanidinobenzimidazole)Br$_3$] (**6b**)*

Anal. Calcd. for $C_8H_9Br_3N_5Sb$: C, 17.90; H, 1.69; N, 13.05. Found: C, 18.32; H, 1.87; N 12.68. IR (KBr, ν/cm^{-1}): 3439 (ν NH_2), 3324 (ν NH), 3071 (ν CH_{ar}), 1691 (ν CC), 1630 (ν CN). LC–MS: *m/z* (calcd) = 538.66 (537.13) (M + 1): ^{1}H NMR (300 MHz, DMSO-d_6): Δ 12.20 (1H, NH), 7.60 (1H, NH), 7.40 (4H, Ar), 7.10 (3H, NH_2 and NH), m.p. 219–220 °C, yield: 53.47%.

*[Sb(2- benzyl-2-thiopseudeourea)$_2$Cl$_3$] (**7a**)*

Anal. Calcd. for $C_{16}H_{18}Cl_3N_4S_2Sb$: C, 34.40; H, 3.25; N, 10.03; S, 11.48. Found: C, 34.77; H, 3.18; N, 10.43; S, 11.97. IR (KBr, ν/cm^{-1}): 3305 (ν NH_2), 3194 (ν NH), 3085 (ν CH_{ar}), 1637 (ν CC_{ar}), 1385 (ν CH). LC–MS: *m/z* (calcd) = 560.59 (559.51) (M + 1). ^{1}H NMR (300 MHz, DMSO-d_6): Δ 4.50 (2H, CH_2S), 7.40 (5H, Ar), 9.30 (2H, NH_2) and 9.10 (1H, NH), m.p. >400 °C, yield: 54.27%.

*[Sb(2-benzyl-2-thiopseudeourea)$_2$Br$_3$] (**7b**)*

Anal. Calcd. for $C_{16}H_{18}Br_3N_4S_2Sb$: C, 27.77; H, 2.62; N; 8.10; S, 9.27. Found: C, 27.22; H, 2.46; N, 7.72; S, 10.08. IR (KBr, ν/cm^{-1}): 3310 (ν NH_2), 3206 (ν NH), 3091 (ν CH_{ar}), 1639 (ν CC_{ar}), 1385 (ν CH). LC–MS: *m/z* (calcd) = 692.94 (692.99) (M+). ^{1}H NMR (300 MHz, DMSO-d_6): Δ 4.50 (2H, CH_2S), 7.40 (5H, Ar), 9.20 (2H, NH_2) and 9.00 (H, NH), m.p. >400 °C, yield: 77.84%.

Glutathione reductase activity

The activity of the glutathione reductase to reduce the GSSG was assayed at 25 °C in phosphate buffer (pH 7.2) by monitoring the oxidation of NADPH at 340 nm. The assays, in a total volume of 3 mL, contained 2×10^{-4} M NADPH (0.08 mmol), 1×10^{-4} M GSSG (0.04 mmol) and 50 μL (1.0 units/mL) of glutathione reductase solution. The reaction was started by addition of the enzyme and the decrease of absorbance was measured at 340 nm at every 30 s [35]. The same process was repeated with different concentrations of the complexes.

DNA cleavage activity

The interactions of the complexes with supercoiled pBR322 plasmid DNA were studied by agarose gel electrophoresis. The complexes were incubated with pBR322 DNA in the dark at 37 °C for 24 h and electrophoresed in 1% agarose gel electrophoresis. The gel was electrophoresed for 3 h at 60 V in 1XTAE buffer. After electrophoresis, the gel was stained in ethidium bromide, then, DNA viewed with UV-transilluminator.

BamH1 and HindIII restriction enzyme digestion

The complex-DNA mixtures were first incubated for 24 h and then restricted with 1 Unit of restriction enzyme *BamH*I and *Hind*III for 1 h at 37 °C. *BamH*I and *Hind*III are known to recognize the sequence G/GATCC and A/AGCTT respectively [36]. pBR322 plasmid DNA contain a single restriction site for each enzymes which convert supercoiled form I DNA and singly nicked circular form II DNA to linear form III DNA. After one hour incubation, the restricted DNA was electrophoresed in 1% agarose gel for 3 h at 60 V in TAE buffer. The gel was stained with ethidium bromide and then viewed with a transilluminator and the image capture by a video-camera as a TIFF file.

Antimicrobial activity

The antibacterial activity of the complexes was performed against American Type Culture Collection (ATCC) reference bacterial strain *Staphylococcus aureus* (ATCC 25923), *Bacillus cereus* (NRLL B-3008), *Bacillus subtilis (*ATCC 29213), *Pseudomonas aeruginosa* (ATCC 27853), *Escherichia coli* (ATCC 35218 resistant to beta lactam antibiotics), *E. coli* (ATCC 25922 resistant to the antibiotics other than beta lactam antibiotics), *Proteus vulgaris* (ATCC 8427) and *Enterobacter fecalis* (ATCC 292112) and fungi *Candida albicans* (ATCC 10231) and *Candida tropicalis* (ATCC 13803) by Agar well diffusion technique. The nutrient agar medium and Sabouraud dextrose agar were poured into Petri dishes after solidification test strain were inoculated in the media. After that a well was made in the Petri dishes by a sterile borer. The complexes (2500 μM) were introduced into the well. Then, all bacterial strain were grown in nutrient agar medium and incubated at 37 °C for 24 h. The yeast strains were grown in Sabouraud dextrose agar medium and incubated at 30 °C for 72 h. Chloramfenicol, Ampicillin (antibacterial) and Ketoconazole (antifungal) were used as standard antibacterial agents. All testings were repeated for three times, and the mean values were calculated.

Computational details

Quantum calculation were carried out using the B3LYP/LANL2DZ (method/basis) by Gaussian 03 W program [37]. All the structures were fully optimized. The absence of imaginary frequencies verified that all structures were true minima. The output files from Gaussian were transferred to the program CODESSA to calculate approximately 350 molecular descriptors (constitutional, topological, geometrical, electrostatic, quantum-chemical). In addition, we have used one indicator parameter for presence (1) and absence (0) of chloro antimony(III) complexes.

For regression analysis, glutathione reductase inhibitor activity values were converted to negative logarithm scale ($pIC_{50} = -\log IC_{50}$) and used as dependent variables. Calculated descriptor values were used as independent variables. Best Multiple Linear

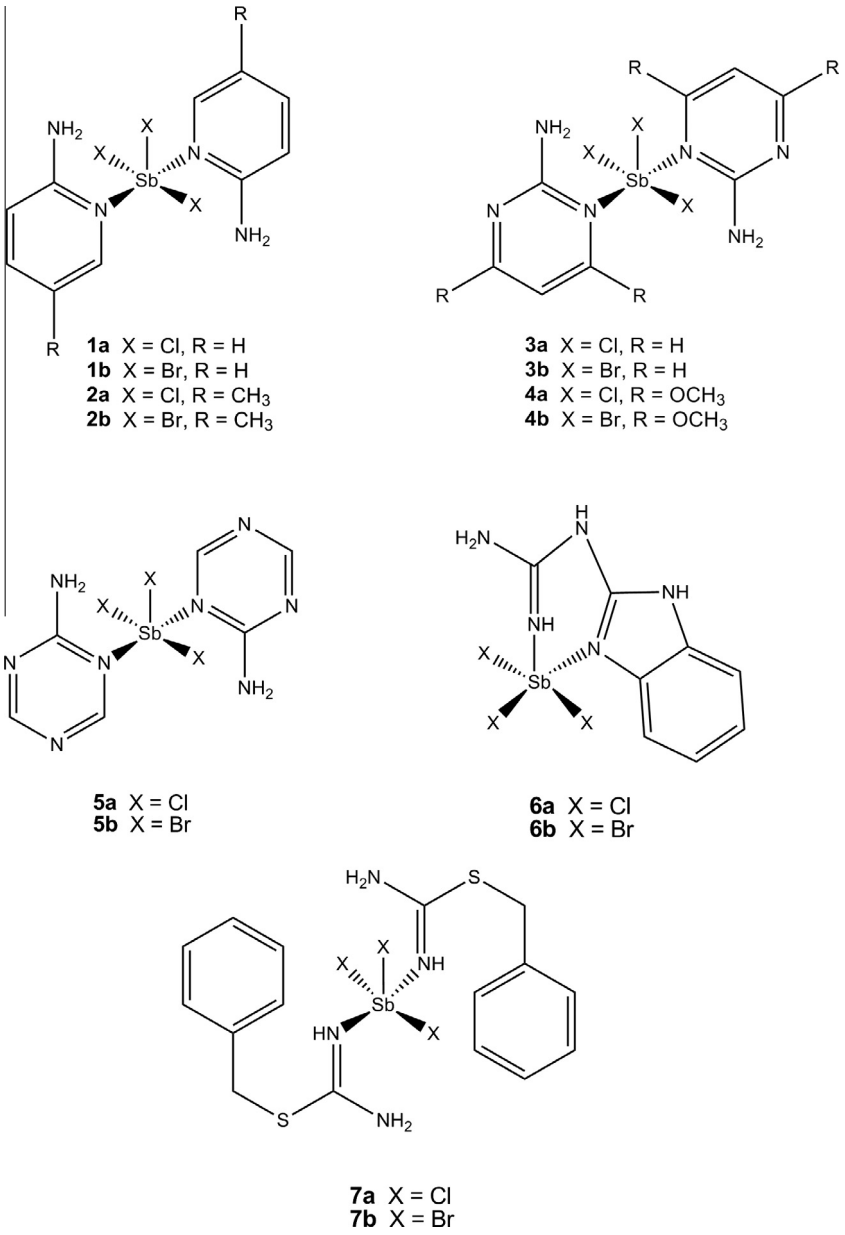

Fig. 1. Structures of the complexes.

Regression method in CODESSA software was used to accomplish the preselection of the descriptors and to build the linear model equation [38].

The "breaking point" rule was applied to determine the optimal number of descriptors in the model equations. This rule is based on the significant improvement of R^2 ($\Delta R^2 < 0.02–0.04$) with respect to the number of descriptors in the model. Consequently, two descriptors were used as independent variables in our models.

The squared correlation coefficient (R^2), leave-one-out cross-validated squared correlation coefficient (R^2cv), the Fisher criteria (F), and standard error (s^2) were used as criteria for the stability and the robustness of the models. The obtained model was also validated with an internal validation method.

Results

Characterization of the complexes

New antimony(III) complexes (Fig. 1) were synthesized as described in Section 'Experimental', and characterized by using elemental analyses, conductometric measurements, LC–MS, FTIR and ^{1}H NMR spectroscopy techniques. The molar conductivity data in DMSO solution show that all complexes are non-electrolyte. According to obtained data, pyridines, pyrimidines and thiopseudourea behaves as monodentate ligands with N donor atom on aromatic ring, however, guanidinobenzimidazole behaves as bidentate ligand with a N donor atom of benzimidazole group and a N donor atom of guanidine moiety. Geometries of all complexes were optimized using DFT/B3LYP/LANL2DZ method/basis set to find most-stable structures. The ground state optimized geometry of all complexes (given in Fig. 2) has square-pyramidal geometry.

Sb(III) complexes with monodentate ligands have a plane with two N donor atoms and two Br atoms in trans arrangement, and one Br atom above the plane (in apical position). However, at the antimony(III) complexes with guanidinobenzimidazole ligand (**6a** and **6b**), Sb(III) atom shares a plane with three bromine atoms and one nitrogen atom of benzimidazole group, and one N donor atom of guanidine moiety above the plane (in *apical* position).

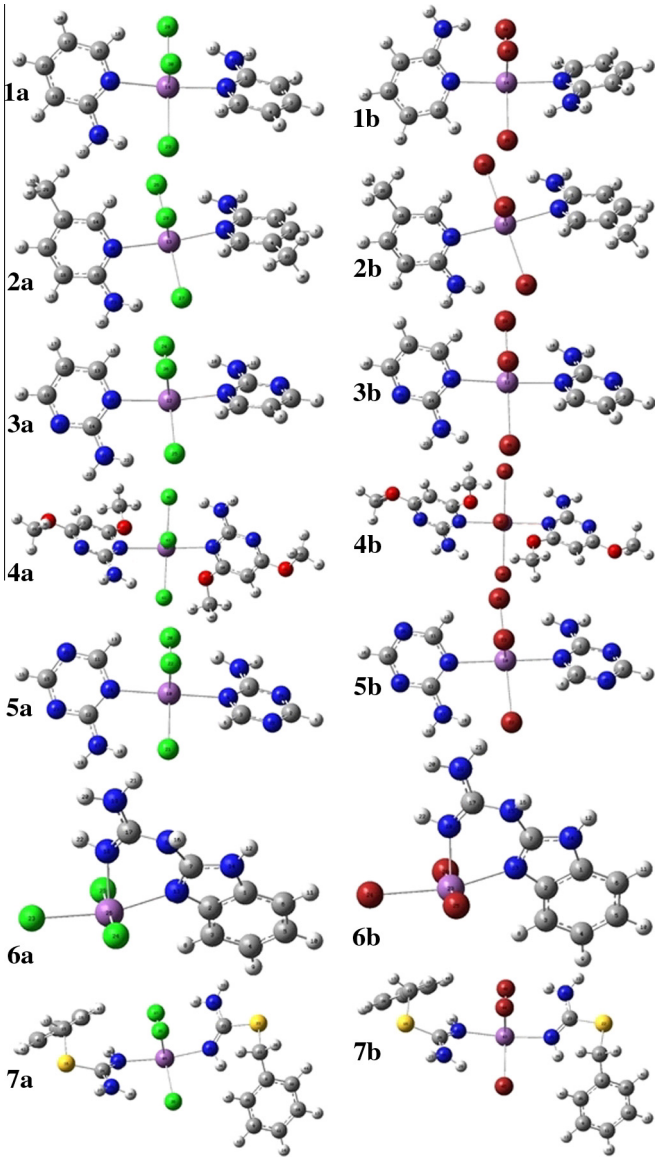

Fig. 2. The ground state optimized structures of the complexes calculated with B3LYP/LANL2DZ method.

IR spectra of complex **1–5** are very similar to each other. In these complexes NH_2 stretching vibrations, found about 3446 cm^{-1} in the free ligand, showed no shifting with complex formation, showing that ligands did not coordinate to the Sb(III) atom via N donor atom of NH_2 substituent on the ring. The ring stretching vibrations of ligands generally shifted to higher wavenumber with complex formation, suggesting that ligands bonded to Sb(III) atom via N donor atoms on aromatic ring. These shifting can be explained by coupling of stretching vibrations of ring with M-N stretching vibration. ν (NH) vibration of guanidinebenzimidazole **(6)** is shifted towards higher wave numbers from 3188 cm^{-1} to 3333 cm^{-1} by complex formation, and ring vibrations of complex **6** showed significant shifting to higher wavenumber suggesting that ligand is bonded via nitrogen atom of guanidine moiety and nitrogen donor atom benzimidazole ring in the complex **6a** and **6b**. However, ν (NH_2) vibration of it showed no shifting with complex formation. ν (NH) vibration of 2-benzyl-2-thiopseudourea is shifted towards higher wave numbers from 3022 cm^{-1} to 3194 cm^{-1} by complex formation, suggesting that ligand is bonded via nitrogen atom of guanidine moiety in the complex **6a** and **6b**. However, ν (NH_2) vibration and ring vibrations of ligand showed no significant shifting with complex formation.

Proton peaks of the ligands **1–5** were shifted to lower field by complex formation. Protons of guanidine moiety of ligand **6** appear as broad singlet at 6.90 ppm and complexation cause a upfield shift about 0.5 ppm. However, NH proton of benzimidazole group of ligand 6 appearing as singlet peak at 11.00 ppm shifted to downfield with complex formation. ^1H NMR spectra of complex **6a** and **7a** were given in Fig. 3. On the other hand, protons of guanidine moiety of ligand **7** appear as singlet at 98.50 ppm, however, complex **7a** show, two well-separated singlets at 9.25 and 9.14 ppm, attributed to the NH_2 and NH protons respectively.

Mass spectra of all complexes, *m/z* values were given at Section 'Experimental', showed molecular ion peak of significant intensity with the characteristic peak pattern of Sb, conforming that all complex were monomeric structure. For example, LC–MS spectra for complex **6a** and **7a** (given in Fig. 3) display the molecular ion peak at *m/z* 404.08 and 560.59 confirming the presence of $SbLCl_3$ and SbL_2Cl_3 molecular formula, respectively.

Inhibition of glutathione reductase

Comparison of IC_{50} values of all complexes (given in Fig. 4) highlights the following facts:

(a) Complex **6b** and **6a** exhibited better glutathione reductase inhibitory activity with IC_{50} value in the range of 4.87–5.87 μM.
(b) In general, bromoantimony(III) complexes showed higher glutathione reductase inhibitory activity than chloroantimony(III) complexes.
(c) Glutathione reductase inhibitor activity of ligands decreases as follows: guanidinobenzimidazole > 2-benzyl-2-thiopseudeourea > triazine > 2-aminopyrimidine > 2-aminopyridine > 5-methylpyridine > 4,6-methoxypyrimidine.
(d) Electron donating substituents on aromatic ring decrease the glutathione reductase inhibitory activity.
(e) More N donor atom on aromatic ring increases the activity.

QSAR analysis

The multilinear regression analysis using Best Multi Linear Regression (BMLR) method for the 14 complexes in the two-parameter model is given in Table 1. In this table, X and ΔX are regression coefficients of the QSAR equation and their standard errors, respectively. The models are given in decreasing relevance order according to their statistical significance (ordered by *t*-test value). A graphical presentation of the relationship between the experimental and the predicted pIC_{50} values for two-parameter QSAR model is given in Fig. 5. Observed and predicted pIC_{50} values, their difference and molecular parameters in the model equation were given in Table 2. In the model equation, first descriptor, "max partial charge for a H atom" computed by Zefirov is an electrostatic descriptor related to charge distribution of H atom [39]. It is related with hydrogen bond and interaction between the cation and anion. Increase in "maximum partial charge for a H" would be favorable for the inhibition of the glutathione reductase activity of the complexes. However, second descriptor, "HOMO–LUMO energy gap" is inversely proportional to the inhibition activity. A low HOMO–LUMO gap implies low stability, easy polarizability for the molecule and also higher reactivity in the chemical reaction. Molecular orbital surfaces of HOMO/LUMO of the complexes were given in Fig. 6.

Absence of collinearity is confirmed by intercorrelation matrix for the independent variables used in our model. No significant correlation was found between two descriptors (−0.0045).

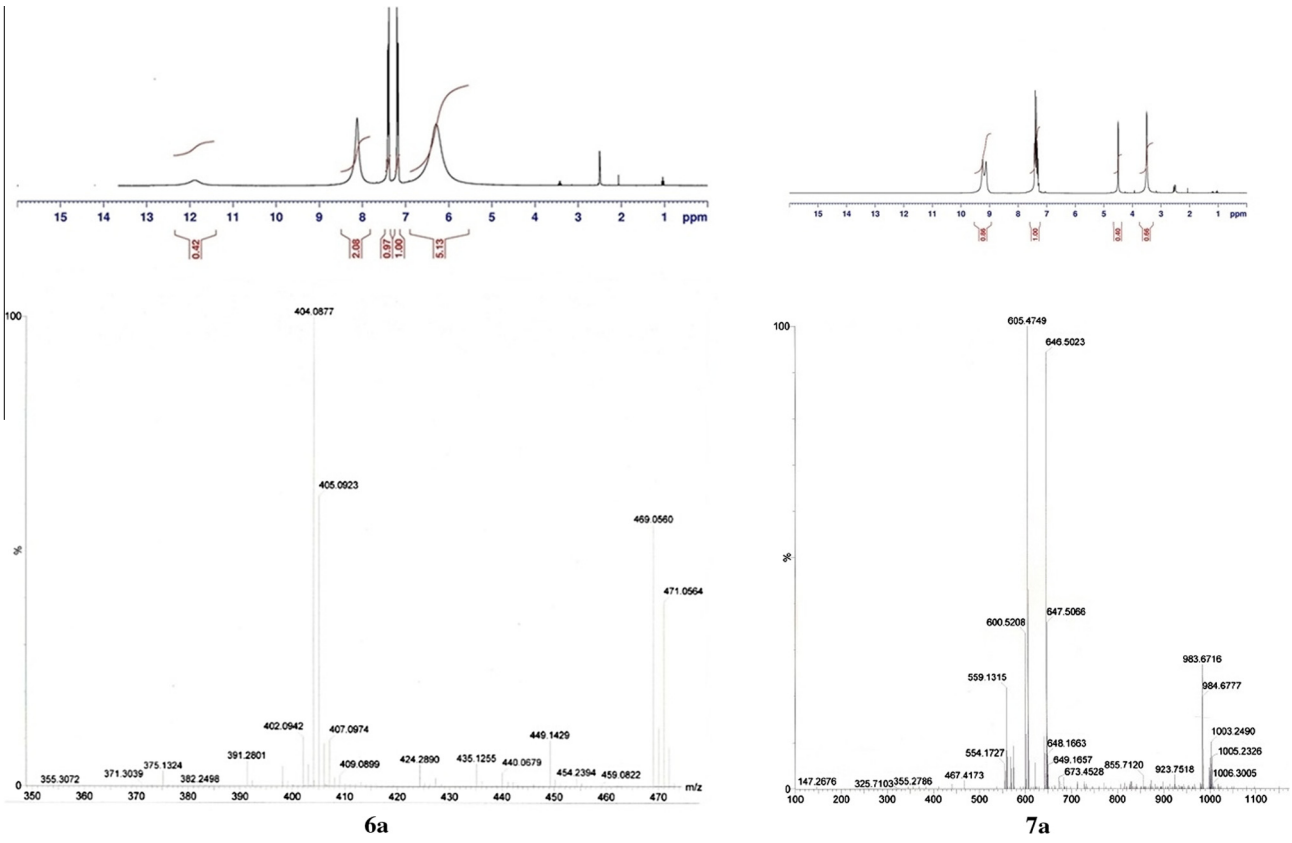

Fig. 3. ^{1}H NMR (above) and LC–MS spectra (below) of complexes **6a** and **7a.**

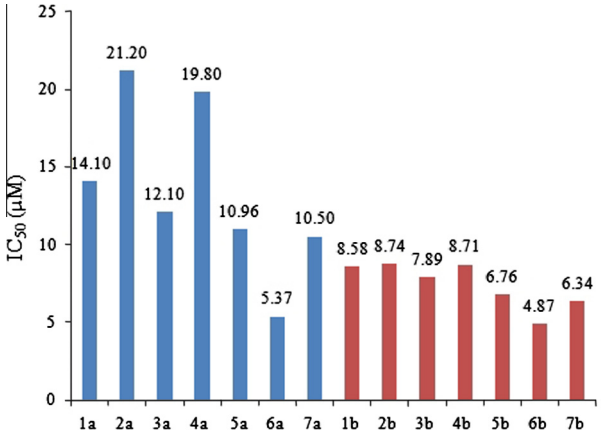

Fig. 4. Experimental IC_{50} values of the complexes.

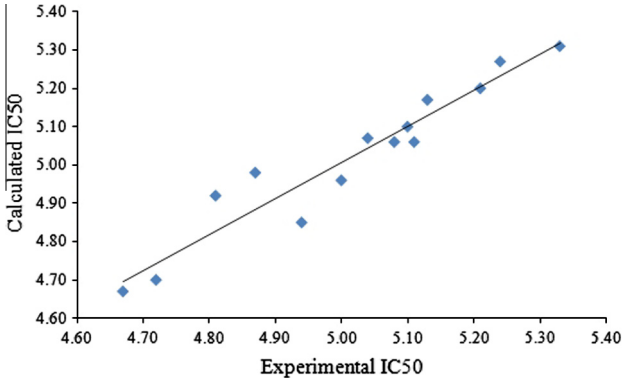

Fig. 5. Correlation of observed and estimated pIC_{50}.

Obtained model equation was further tested with an internal validation method (given in Table 3). For this method, initially, the full set of the 14 structures was sorted in ascending order according to the pIC_{50} value and then divided into three subsets A, B and C: the first, fourth, seventh structure, etc., formed subset (A); the second, fifth, eight, etc. formed subset (B); and the third, sixth, ninth structure, etc. formed subset (C). Then, these three sets A–C were prepared as the combination of two training subsets (A + B), (A + C) and (B + C). The remaining subsets (C, B and A, respectively) become the corresponding test sets. As seen in Table 3, the

Table 1
The inhibitor activity and molecular parameters of the complexes.

	X	X	*t*-test	Descriptor
0	-4.3628×10^{-1}	2.7721×10^{-1}	−1.5738	Intercept
1	1.9176×10^{1}	3.3571	8.7121	Max partial charge for a H atom
2	-3.8932×10^{-1}	4.6510×10^{-2}	−5.3707	HOMO–LUMO energy gap
$n = 14$	$R^2 = 0.9133$	$F = 57.96$	$s^2 = 0.0038$	$R^2_{cv} = 0.8546$

Table 2
DFT-based two parameters QSAR model equation by BMLR method.

Compound no.	Inhibitor activity			Descriptors			
	pIC_{50} (exp)	pIC_{50} (calc)	$\Delta_{Obs\text{-}pred.}$	MPCH[a]	E_{HOMO}	E_{LUMO}	$\Delta E_{HOMO-LUMO}$
1a	4.85	4.94	−0.09	0.0483	−6.4595	−1.9884	4.4711
2a	4.67	4.67	0.00	0.0483	−6.2453	−2.5288	3.7166
3a	4.91	4.81	0.10	0.0484	−6.2981	−1.8909	3.7362
4a	4.70	4.72	−0.02	0.0484	−6.1545	−2.4183	3.6749
5a	4.96	5.00	−0.04	0.0522	−6.7860	−2.4368	4.3492
6a	5.27	5.24	0.03	0.0522	−6.5379	4.3492	4.5898
7a	4.97	4.87	0.10	0.0539	−6.2472	−2.8629	4.5898
1b	5.07	5.04	0.03	0.0539	−5.9727	−1.6575	3.8687
2b	5.05	5.08	−0.03	0.0531	−7.1945	−2.9095	4.2850
3b	5.10	5.10	−0.00	0.0531	−6.8829	−3.2414	3.6415
4b	5.06	5.11	−0.05	0.0619	−5.9836	−2.0452	3.9383
5b	5.17	5.13	0.04	0.0619	−5.8695	−2.2548	3.6148
6b	5.31	5.33	−0.02	0.0603	−6.3868	−1.8485	4.5384
7b	5.19	5.21	0.02	0.0603	−6.2342	−2.3764	3.8578

[a] MPCH: max partial charge for a H atom.

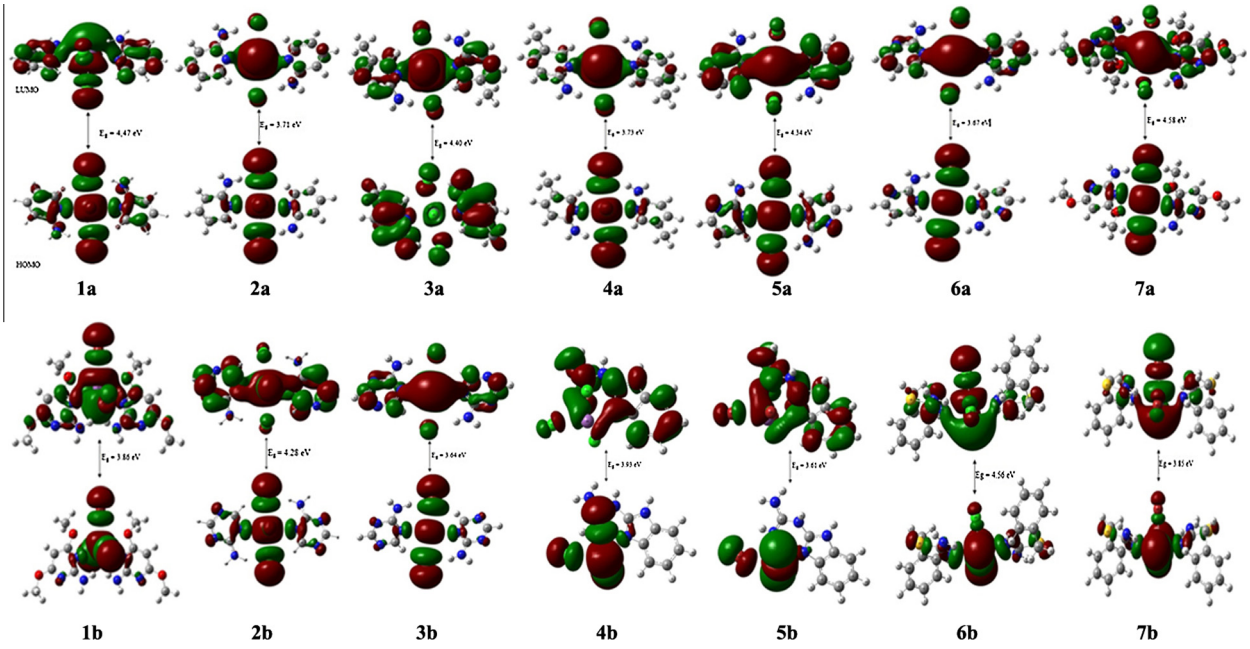

Fig. 6. Molecular orbital surface for the HOMO and LUMO of complexes.

Table 3
Internal validation of the QSAR model.

Training set	*N*	R^2	R^2cv	*F*	s^2	Test set	*N*	R^2
A + B	10	0.9873	0.9725	255.17	0.0070	C	4	0.9811
A + C	9	0.9765	0.9414	283.14	0.0086	B	5	0.9582
B + C	9	0.9924	0.9745	261.61	0.0116	A	5	0.9443

minimum training quality of R^2 0.9765 and a minimum predicting quality of 0.9443 demonstrate that the proposed model has a satisfactory statistical stability and validity.

DNA cleavage activity

Change in the mobility of plasmid DNA on agarose gel is commonly taken as evidence for direct DNA-metal interactions. In an attempt to gain insight into the anti-leishmanial mechanism of action of complexes, DNA cleavage activity was investigated by gel electrophoresis. It is well-known that some drugs bind DNA, changes DNA conformation and damage the DNA. As a result of these changes, the rate of DNA migration in an electric field may change. Plasmid DNA can exist in three forms: as supercoiled circular (Form I), singly nicked relaxed (Form II), and double nicked linear (Form III). Supercoiled form DNA (Form I, SC) migrates faster on the gel than nicked circular DNA (Form II, NC). If one strand is cleaved, the supercoils will relax to produce a slower moving open circular form (Form II), if both strands are cleaved, a linear form (Form III) that migrates in between will be generated. In order to determine whether the complexes cause conformational changes and/or damage to plasmid DNA helix, we studied the complexes

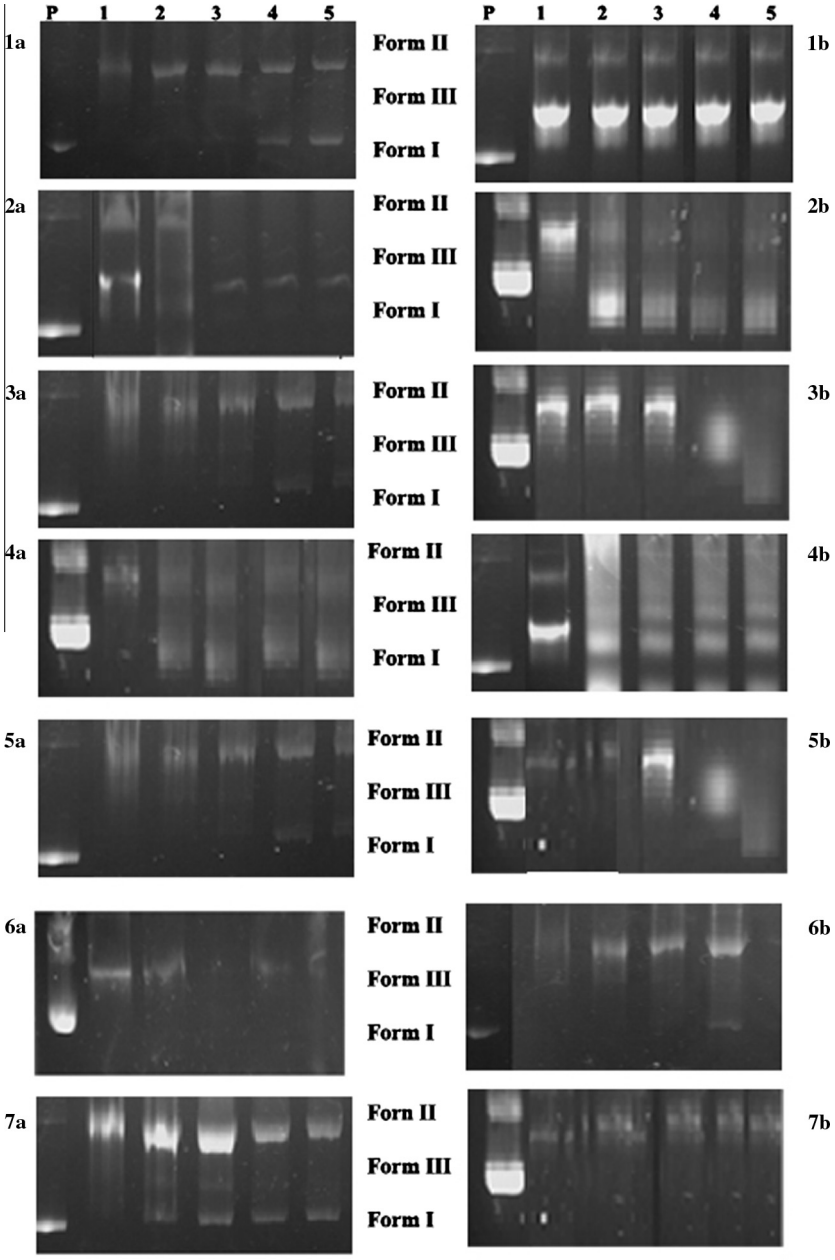

Fig. 7. Electrophoretograms applied to the incubated mixtures of Plasmid DNA (P) and varying concentrations of the compounds (lane 1: 5000 μM, lane 2: 2500 μM, lane 3: 1250 μM, lane 4: 625 μM, line 5: 312.5 μM).

capacity to induce single or double strand breakage of closely circular DNA.

Fig. 7 gives the electrophoretograms applying incubated mixtures of plasmid DNA and varying concentrations of the complexes (5000 μM, 2500 μM, 1250 μM, 625 μM, 312.5 μM) after 24 h. Line P applies untreated plasmid DNA as a control. Lines 1–5 apply to plasmid DNA incubated with decreasing concentrations of the complexes. Compared with DNA control (Lane P), the patterns of Lanes 2–5, demonstrate that all the complexes are found to exhibit nuclease activity, because all complexes cause conformational changes in form I plasmid DNA. The conversion of supercoiled form (Form I, SC) to nicked form (Form II, NC) becomes more efficient with increasing concentration of complexes **6b**, **5b**, **3b** and **4b**, and the emergence of Form III predicts double strand DNA cleavage. Remaining complexes show that DNA was converted from supercoiled form (Form I) to nicked circular form (Form II) without further conversion to linear form (Form III), predicting single strand DNA cleavage. Based upon their ability to convert supercoiled form (Form I, SC) to nicked circular form (Form II, NC) and then to linear open circular DNA form (Form III, LC), the tendency of the complexes varies as **6b** ∼ **5b** > **3b** > **4b**.

Restriction enzymes cut DNA at or near specific recognition nucleotide sequences known as restriction sites [40]. *BamH*I and *Hind*III are known to recognize the sequences G/GATCC and A/AGCTT respectively [36]. pBR322 plasmid DNA contain a single restriction site for each enzyme which convert supercoiled form I DNA and singly nicked circular form II DNA to linear form III DNA.

Fig. 8 gives electrophoretograms of plasmid/complexes restricted *with Bam*HI enzymes. Lane P applies to untreated and undigested plasmid DNA. Lane P/B applies untreated but digested DNA with *BamH*I enzyme, line 1 4 applied to pBR322 plasmid DNA interacted with complexes **6b**, **6a**, **5a** and **3a** followed by

Table 4
Inhibition zones (in mm) of the compounds and reference antibiotics discs against tested microorganisms by disc diffusion method.

Comp.	*B. subtilis*	*B. cereus*	*E. fecalis*	*S. aureus*	*K. pneumoniae*	*E. coli* 35218	*E. coli* 25922	*P. aeroginosa*	*C. albicans*	*C. tropicalis*	*C. krusei*
1a	29.00 ± 0.57	26.00 ± 1.00	–	–	–	–	–	18.50 ± 0.70	–	–	–
2a	26.00 ± 1.00	25.00 ± 1.00	–	–	–	–	–	13.00 ± 1.00	–	–	–
3a	30.00 ± 0.57	25.50 ± 0.70	–	–	–	–	–	18.00 ± 0.40	–	–	–
4a	18.00 ± 1.00	20.00 ± 1.00	–	–	–	–	–	14.00 ± 1.00	–	–	–
5a	31.00 ± 0.57	26.50 ± 0.70	–	–	19.00 ± 1.00	20.00 ± 0.00	18.00 ± 0.00	18.00 ± 0.40	–	–	–
6a	33.33 ± 1.00	30.00 ± 1.00	–	–	25.00 ± 0.00	23.67 ± 0.57	20.00 ± 0.56	19.67 ± 0.57	–	–	–
7a	33.00 ± 1.00	29.67 ± 1.10	–	–	20.00 ± 1.00	22.67 ± 0.70	19.10 ± 1.00	18.67 ± 0.57	–	–	–
1b	26.00 ± 1.00	26.00 ± 1.00	–	–	–	–	–	12.00 ± 1.00	–	–	–
2b	25.00 ± 1.00	24.00 ± 1.00	–	–	–	–	–	11.00 ± 1.00	–	–	–
3b	26.50 ± 0.70	26.00 ± 1.00	–	–	–	–	–	11.00 ± 1.00	–	–	–
4b	17.00 ± 1.00	19.00 ± 1.00	–	–	–	–	–	12.00 ± 1.00	–	–	–
5b	27.50 ± 0.70	26.50 ± 1.00	–	–	18.00 ± 1.00	18.00 ± 0.00	17.00 ± 0.00		–	–	–
6b	30.00 ± 1.00	28.50 ± 0.70	–	–	21.00 ± 1.00	22.50 ± 0.70	19.00 ± 0.56	14.00 ± 1.00	–	–	–
7b	26.00 ± 1.00	27.00 ± 1.00	–	–	19.00 ± 1.00	22.00 ± 1.00	18.00 ± 1.00	13.00 ± 1.00	–	–	–
A[a]	23.00 ± 1.00	–	27.00 ± 1.00	44.00 ± 1.00	–	–	18.00 ± 1.00	60.00 ± 0.50	–	–	–
C[a]	21.00 ± 0.50	–	20.00 ± 0.51	24.00 ± 1.00	31.00 ± 0.53	8.00 ± 0.52	25.00 ± 0.56	34.00 ± 0.52	–	–	–
K[a]	–	–	–	–	–	–	–	–	11 ± 1	34 ± 2	18 ± 1

[a] A: Ampicillin, 10 g (2.86×10^{-8} mole), C: Chloramfenicol, 30 g (9.28×10^{-8} mole), Ketoconazole 0.5 mg/mL (9.40×10^{-7} mole).

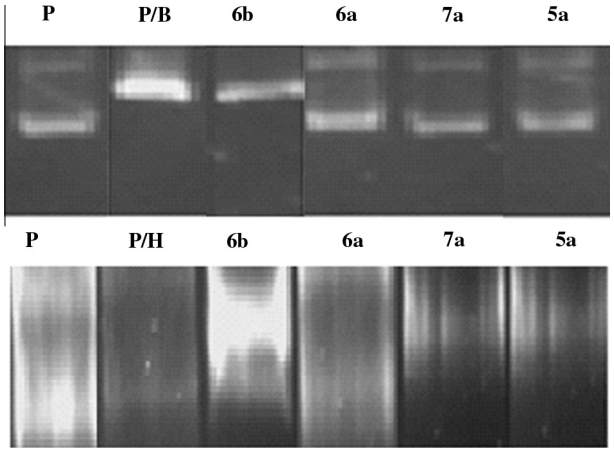

Fig. 8. Electrophoretograms for the *Bam*HI (*up*) and *Hind*III (*down*) digested mixtures of pBR322 plasmid DNA after their treatment with various concentrations of compounds. (lane P, untreated pBR322 plasmid DNA, and P/B, P/H; pBR322 DNA linearized by *BamH*I and *Hind*III, respectively.)

*Bam*HI digestion. In our study, DNA complexes mixtures were digested with *BamH*I and *Hind*III enzymes. When plasmid DNA interacted with complexes **1a**, **3a**, **5a** and **6a** followed by *BamH*I digestion, two bands were observed for **3a**, **6b**, **5a** except **6a.** The prevention of restriction enzyme *BamH*I digestion means that DNA conformation is changed by the complexes interaction. When plasmid DNA interacted with the same complexes followed by *Hind*III digestion, only one band was observed for all of the complexes tested except **6a**. Complex **6b** binds GG and AA bases of DNA. Additionally, complexes **5a** binds to AT bases, however, complexes **6a** and **3a** bind to GG bases of DNA.

In vitro antimicrobial activity

All complexes were tested for their in vitro antimicrobial activity against some bacteria and fungi (Table 4). At even higher concentrations, none of the complexes showed antifungal activity against *C. albicans C. tropicalis* and *C. krusei.* We were surprised because, dichloroantimony(III) pyrazolinates [41] and antimony(III) carboxylates [42] were reported to exhibit antifungal activity, implying that antifungal activity of antimony(III) complexes depends on type of ligands.

All compounds displayed strong antibacterial activity against, *B cereus, B. subtilis* and *P. aeruginosa*. Compounds **5a**, **6a, 7a 5b, 6b** and **7b** showed moderate antibacterial activity against *K. pneumoniae, E. coli 35218* and *E. coli* 25922. Particularly, the activity of compound **6a** against *B. cereus* was comparable or higher than that of the standard drugs (chloramfenicol and ampicillin). It was expected because benzimidazole derivatives and their complexes exhibit various bioactivities including antimicrobial activities [43,44]. In general, it can be concluded that antibacterial activity of trichloroantimony(III) complexes have higher than the tribromoantimony(III) complexes.

Conclusion

In this paper, we report the glutathione reductase inhibitory activity, DNA-cleavage activity and antimicrobial activity of new fourteen antimony(III) complexes. Guanidinobenzimidazol and thiopseudourea Sb(III) complexes showed good biochemical activity. Glutathione reductase inhibitory activity and DNA-cleavage activity of bromo antimony complexes are significantly more potent than that of chloro antimony complexes, however, chloro antimony complexes show more antimicrobial activity than bromo antimony complexes. The cleavage of plasmid pBR322 DNA experiments show that all our antimony(III) complexes serve as metallonucleases. **6b** complex behaves as an efficient chemical nuclease for double-strand cleavage of DNA, and binds both G/G and A/A bases. Two-parameter QSAR model for glutathione reductase inhibitory activity of fourteen antimony(III) complexes show that decrease in "maximum partial charge for a H" and HOMO–LUMO gap would be favorable for the glutathione reductase inhibitory activity.

Acknowledgements

This work has been supported in part by The Scientific and Technological Research Council of Turkey (TUBITAK) Project no: 212T089 and by Russian Foundation for Basic Research. We are grateful to Prof. Dr. Ningur Noyanalpan for helpful comments.

References

[1] A. Meister, M.E. Anderson, Glutathione, Ann. Rev. Biochem. 52 (1983) 711–760.
[2] C. Biot, H. Bauer, R.H. Schirmer, E. Davioud-Charvet, J. Med. Chem. 47 (2004) 5972–5983.
[3] S. Wyllie, A.H. Fairlamb, Biochem. Pharm. 71 (2006) 257–267.

[4] T. Muller, L. Johann, B. Jannack, M. Bruckner, D.A. Lanfranchi, H. Bauer, C. Sanchez, V. Yardley, C. Deregnaucourt, J. Schrevel, M. Lanzer, R.H. Schirmer, E. Davioud-Charvet, J. Am. Chem. Soc. 133 (2011) 11557–11571.
[5] A. Citta, E. Schuh, F. Mohr, A. Folda, M.L. Massimino, A. Bindoli, A. Casini, M.P. Rigobello, Metallomics 5 (2013) 1006–1015.
[6] N. Chavain, E.D. Charvet, X. Trivelli, L. Mbeki, M. Rottmann, R. Brun, C. Bioorg, Med. Chem. 17 (2009) 8048–8059.
[7] M.A.L. Blackie, A. Saravanamuthu, A.H. Fairlamb, K. Chibale, Arkivoc 6 (2008) 52–60.
[8] A. Casini, J. Reedijk, Chem. Sci. 3 (2012) 3135–3144.
[9] A. Panja, Polyhedron 43 (2012) 22–30.
[10] C.-L. Liu, M. Wang, T.-L. Zhang, H.-Z. Sun, Coord. Chem. Rev. 248 (2004) 147.
[11] F. Perveen, R. Qureshi, A. Shah, S. Ahmed, F.L. Ansari, S. Kalsoom, S. Mehboob, Int. Res. J. Pharm. 1 (2011) 1–8.
[12] X. Wang, H. Sun, Comprehensive Inorganic Chemistry II, second ed., 2013.
[13] M. Navarro, C. Gabbiani, L. Messori, D. Gambino, Drug Discov. Today 15 (2010) 1070–1078.
[14] T. Newlove, L.H. Guimarães, D.J. Morgan, L. Alcântara, M.J. Glesby, E.M. Carvalho, P.R. Machado, Am. J. Trop. Med. Hyg. 84 (2011) 551–555.
[15] Y.Z. Voloshin, O.A. Varzatskii, Y.N. Bubnov, Russ. Chem. B+ 56 (2007) 577–605.
[16] G.L. Parrilha, R.P. Dias, W.R. Rocha, I.C. Mendes, D. Benítez, J. Varela, H. Cerecetto, M. González, C.M.L. Melo, J.K.A.L. Neves, V.R.A. Pereira, H. Beraldo, Polyhedron 31 (2012) 614–621.
[17] I.I. Ozturk, C.N. Banti, M.J. Manos, A.J. Tasiopoulos, N. Kourkoumelis, K. Charalabopoulos, S.K. Hadjikakou, J. Inorg. Biochem. 109 (2012) 57–65.
[18] S.K. Hadjikakou, I.I. Ozturk, M.N. Xanthopoulou, P.C. Zachariadis, S. Zartilas, S. Karkabounas, N. Hadjiliadis, J. Inorg. Biochem. 102 (2008) 1007–1015.
[19] B.M. Day, Martyn P. Coles, Peter B. Hitchcock, Eur. J. Inorg. Chem. 5 (2012) 841–846.
[20] I.I. Ozturk, O.S. Urgut, C.N. Banti, N. Kourkoumelis, A.M. Owczarzak, M. Kubicki, S.K. Hadjikakou, Polyhedron 70 (2014) 172–179.
[21] F. Frezard, P.S. Martins, M.C.M. Barbosa, A.M.C. Pimenta, W.A. Ferreira, J.E. Melo, J.B. Mangrum, C. Demicheli, J. Inorg. Biochem. 102 (2008) 656–665.
[22] A.J. Magill, Hunter's Tropical Medicine and Emerging Infectious Disease, ninth ed., Leishmaniasis, 2013. pp. 739–760.
[23] M.I. Khan, S. Gul, I. Hussain, M.A. Khan, M. Ashfaq, I.U. Rahman, F. Ullah, G.F. Durrani, I.B. Baloch, R. Naz, Org. Med. Chem. Lett. 1:2 (2011) 1:2.
[24] H.P.S. Chauhan, A. Bakshi, S. Bhatiya, Spectrochim. Acta Part (A) 81 (2011) 417–423.
[25] N.V. Sawant, J.B. Biswal, S.S. Garje, J. Coord. Chem. 64 (2011) 1758–1769.
[26] N.M. El-Metwaly, Moamen S. Refat, Spectrochim. Acta Part (A) 81 (2011) 519–528.
[27] U.N. Tripathi, J.S. Solankiz, M.S. Ahmadz, A. Bhardwaj, J. Coord. Chem. 62 (2009) 636–644.
[28] K. Mahajan, M. Swami, R.V. Singh, Russ. J. Coord. Chem. 35 (2009) 179–185.
[29] C. Hansch, A. Leo, Exploring QSAR: Fundamentals and Applications in Chemistry and Biology, American Chemical Society, Washington, Academic Press Inc., 1995. Copyright © 1994.
[30] N. Ozbek, S. Alyar, H. Alyar, E. Şahin, N. Karacan, Spectrochim. Acta Part (A) 108 (2013) 123–132.
[31] H.G. Aslan, N. Karacan, Med. Chem. Res. 22 (2013) 1330–1338.
[32] H.G. Aslan, S. Ozcan, N. Karacan, Spectrochim. Acta Part (A) 98 (2013) 329–336.
[33] M.S. Karacan, C. Yakan, M. Yakan, N. Karacan, S.K. Zharmukhamedov, A. Shitov, D.A. Los, V.V. Klimov, S.I. Allakhverdiev, Biochim. Biophys. Acta 187 (2012) 1229–1236.
[34] S. Alyar, N. Ozbek, K. Kuzukıran, N. Karacan, Med. Chem. Res. 20 (2011) 175–183.
[35] M.L. Cunningham, M.J.J.M. Zvelebil, A.H. Fairlamb, Eur. J. Biochem. 221 (1994) 285–295.
[36] R.J. Roberts, G.A. Wilson, F.E. Young, Nature 265 (1977) 82–84.
[37] M.J. Frisch et al., Gaussian Inc, Pittsburgh PA., Gaussian 03 (Revision B.04), 2003.
[38] A. Katritsky, M. Karelson, V.S. Lobanov, R. Dennington, T. Keith, CODESSA 2.7.10, Semichem Inc., Shawnee, KS, 2004.
[39] A.R. Katritzky, T. Tamm, Y. Wang, S. Sild, M. Karelson, J. Chem. Inf. Comput. Sci. 39 (1999) 684–691.
[40] R.J. Roberts, K. Murray, Crit. Rev. Biochem. 4 (1976) 123–164.
[41] U.N. Tripathi, J.S. Solanki, M.S. Ahmad, A. Bhardwaj, J. Coord. Chem. 62 (2009) 636–644.
[42] F. Montrichard, F. Le Guen, D.L. Martin, E.D. Charvet, FEBS Lett. 442 (1999) 29–33.
[43] H.Z. Zhang, G.L.V. Damu, G. X Cai, C. H Zhou, Eur. J. Med. Chem. 64 (2013) 329–344.
[44] T. Abdel Ghani, Ahmed.M. Mansour, Spectrochim. Acta Part A Mol. Biomol. Spectrosc. 86 (2012) 605–613.